Detection and Localization of Unmodeled Manipulator Collisions*

Scott K. Ralph Dinesh K. Pai
Department of Computer Science
University of British Columbia
Vancouver, Canada
{ralph|pai}@cs.ubc.ca

Abstract

Robotic tasks usually require some collision free motions, and there has been considerable work in methods for collision avoidance. However, noise in the sensor data, movement of the obstacles, and incomplete or inaccurate model of the surroundings all may lead to unexpected collisions. Detecting such collisions is necessary before recovery and/or replanning may take place.

A means of detecting a collision, as well as the position of the collision on the manipulator has been developed. The detection scheme combines information from observed disturbance torques to detect collision and infer the location of contact with the environment. Knowledge of contact position allows for a more intelligent and less error-prone recovery scheme.

A simulation using a three DOF manipulator shows that the collision identification and localization scheme is feasible and robust with respect to noise.

1 Introduction

There has been considerable work in planning robot motions to avoid collision [2, 3, 7]. While we may construct a path which successfully avoids collisions with known obstacles, the problem of unexpected collisions always exists as long as there is uncertainty in our sensing, control, or our modeling of the environment. This is particularly true for mobile robotics where the errors in position may increase as the robot moves in the environment [9].

We propose a method for collision identification and localization using observed disturbance torques at the joints. The disturbance torques provide a great deal of information about the interaction of the manipulator with the environment, with little or no additional sensing.

The method we propose models interactions between surfaces of the manipulator and points in the environment as a set of *features* which are configuration independent. These features have associated parameters which provide a basis for the set of all generalized forces generated by the given feature. Combining these features, with knowledge of the disturbance torques and the manipulator configuration yields a system which is sufficient for identification and localization of collisions of the manipulator with the environment. Localization of the collision involves solving for feature parameters which best fit the observed disturbance torques.

We demonstrate how additional constraints on the system yield an overconstrained system, and a least-squares solution provides a means of determining feature parameters which is robust with respect to noise. We also give a measure based on the least-square projection which provides a useful measure for comparing the merits of competing collision hypotheses.

We will assume below that the disturbance torque τ_d can be estimated with some uncertainty. This could be done by joint torque measurements if we have a model of the actuator dynamics, or measuring joint states and using a disturbance observer [13]. In general we are given a n_d-link manipulator whose equations of motion are described by:

$$\tau_d = M(\theta)\ddot{\theta} + V(\dot{\theta}, \theta) + G(\theta) - \tau_{\text{input}} \quad (1)$$

where M is the mass matrix, V denotes velocity-dependent terms such as the centrifugal and coriolis terms and viscous friction, G denotes position-dependent terms, e.g., due to gravity, τ_{input} represents the inputs to the system, and τ_d represents a disturbance torque. Given measurements or estimates of $\theta, \dot{\theta}$ and $\ddot{\theta}$ we may observe the disturbance torque τ_d.

There have been advances in path planning which deal with uncertain control and sensing [8], as well as path planning which is guaranteed to succeed or noticeably fail [4]. Much less attention has been given to the task of collision detection and localization as a source of information for recovery from unexpected errors. We propose a means by which we may combine knowledge of the sensor and actuator histories, with a model of the dynamics to infer the geometry of contact with the obstacle.

*This work was supported in part by NSERC, IRIS, and the BC ASI.

0-8186-7108-4/95 $4.00 © 1995 IEEE

Proceedings of the International Conference on Intelligent Robots and Systems (IROS '95)
0-8186-7108-4/95 $10.00 © 1995 IEEE

The use of contact information is prevalent in grasping (e.g., [12]), mobile robotics (e.g., [9]), and industrial robotics (e.g., [13]). [12] uses force information from strain gauges to infer interactions with the end effectors and the object. Here the object's position is relatively well known, and it is the position and orientation of the various contacts that are recovered. [9] uses contact information to reduce the uncertainty of the robot's position and orientation. The contact serves as a reference point for the robot. [13] uses a model of the dynamics of a serial manipulator and infers collision when a disturbance of sufficient magnitude occurs.

The overall goal of our approach is similar to the force-based contact sensing of [5, 1], and the contact detection given in [13]. Unlike the work of [13], we wish to extract contact position information, rather than the presence or absence of a collision. We extend the work of [5, 1] to include links with arbitrary geometry, and multiple contact features. This is achieved by explicitly forming the basis of external forces which may act on the manipulator given the geometry of the link, and the contact type. Additionally, the tasks of contact identification and localization are combined into one formalism. Like [13] we may estimate the disturbance torques by observing the system dynamics, or we may use direct measurements of the forces and moments as in [12] if this sensor information is available.

Sensing issues aside, the problem we wish to address is, to a large extent, the inverse problem of [12]. The grasping problem of [12] involves precise knowledge of the object, both position and orientation, with unknown contact geometry. The goal is to infer the contact geometry from measurements of the applied forces and torques at the contacts. With the collision localization problem we use a model of the contact, with measured interaction forces, and infer the unknown position of the object.

We propose a means by which not only the presence of a collision, but also the position of the collision on the manipulator can be inferred. [13] assumes that once a collision has taken place the robot is able to return to a "safe position". This not simple in practice since the same positional errors in the robot that may have lead to the collision may make it impossible to move to the safe position. By recovering the collision geometry we may make a more intelligent choice for error recovery.

We begin in §2 with a description of contact forces on a serial manipulator in terms of features of the links, and their associated parameters. These features are combined with the configuration-dependent terms to produce a contact Jacobian which will fully describe the set of joint forces observable by the manipulator. The task of localizing the collision from a set of disturbance torques is presented in §3. Geometric constraints on the position, as well as cone-constraints due to friction are given to further constrain the system. A means of qualitatively determining which feature took part in the collision, as well as metric for comparing competing contact hypotheses is then developed. Results of a simulation of a planar 3 DOF manipulator is presented in §4, followed by a discussion of possible extensions to the formulation in §5. We conclude with a summary of the results in §6.

2 Contact Forces

Determining contact position involves finding a position and force which is consistent with the observed disturbance torques. Since there will be errors in our disturbance torque measurements, the contact information should correspond to the interpretation which "best" describes the measurements. To sufficiently constrain the system we may have to impose additional constraints on the number and the type of contacts which are modeled.

To model the interaction of the manipulator with an object, we will consider a set of *features* which describe the set of generalized forces which can be transmitted to the manipulator. These features may be generate by point, line, or soft-finger contacts and may include frictional forces (see, for example, [10]).

For example, consider the simplified example of a three DOF manipulator with parallel joints in Fig. 1, with triangular links. The manipulator is effectively planar, but we shall treat it as a spatial manipulator for consistency. Suppose there is frictionless contact between face i of Link$_j$ and a point in the environment. Then the contact wrench (i.e., force and torque) in Link$_j$'s frame of reference is

$$ {}^j w_i \in \mathbb{R}^6 \quad = \quad \lambda_{i1} \begin{pmatrix} \eta_i \\ 0 \end{pmatrix} + \lambda_{i2} \begin{pmatrix} 0 \\ \nu_i \times \eta_i \end{pmatrix} \quad (2) $$

Here λ_{i1} is the magnitude of the contact force, $\eta_i \in \mathbb{R}^3$ is the unit vector normal to face i, $\nu_i \in \mathbb{R}^3$ is a unit vector tangent to face i in the plane perpendicular to the joint axes (since this is effectively a planar problem), and $\lambda_{i2}/\lambda_{i1}$ parameterizes the location of the contact on face i. Thus associated with each feature is a vector λ_i whose elements parameterize the set of possible generalized forces the feature may produce.

$$ \lambda_i \quad = \quad \begin{pmatrix} \lambda_{i1} \\ \lambda_{i2} \end{pmatrix} \quad (3) $$

It is important to note that the λ_i are subject to further admissibility constraints; e.g., λ_{i1} is required to be non-positive since it represents the inward contact force, and λ_{i2} is subject to constraints from the geometry of the face i. We will return to this issue in §3.

The set of all possible contact forces can be expressed in a single configuration independent matrix

Proceedings of the International Conference on Intelligent Robots and Systems (IROS '95)
0-8186-7108-4/95 $10.00 © 1995 IEEE

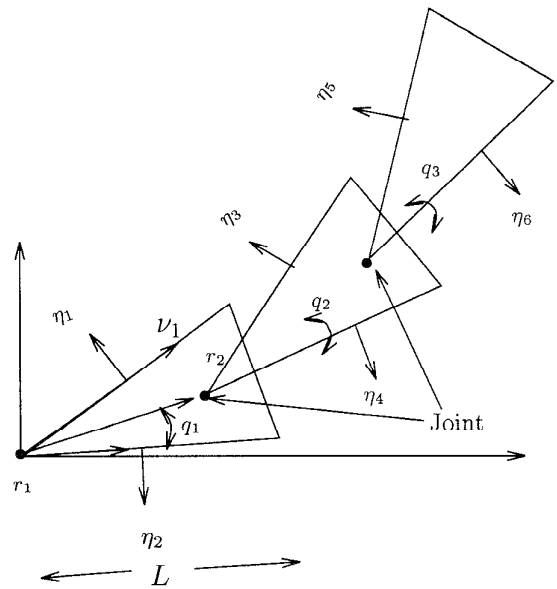

Figure 1: A three DOF planar manipulator with triangular faces.

$F \in \mathbb{R}^{6n_d \times n_f}$, where n_d is the number of degrees of freedom of the manipulator, and n_f is the number of contact features.

For the example suppose the potential contacts between points in the environment and faces of the links can be described by six features shown in Figure 1, one for each face i whose normals are given by η_i.

$$F = \begin{bmatrix} \eta_1 & 0 & \eta_2 & 0 & 0 & 0 & 0 & 0 & 0 & 0 & 0 & 0 \\ 0 & z_1 & 0 & z_2 & 0 & 0 & 0 & 0 & 0 & 0 & 0 & 0 \\ 0 & 0 & 0 & 0 & \eta_3 & 0 & \eta_4 & 0 & 0 & 0 & 0 & 0 \\ 0 & 0 & 0 & 0 & 0 & z_3 & 0 & z_4 & 0 & 0 & 0 & 0 \\ 0 & 0 & 0 & 0 & 0 & 0 & 0 & 0 & \eta_5 & 0 & \eta_6 & 0 \\ 0 & 0 & 0 & 0 & 0 & 0 & 0 & 0 & 0 & z_5 & 0 & z_6 \end{bmatrix}$$

$$\lambda = \begin{pmatrix} \lambda_1 \\ \vdots \\ \lambda_6 \end{pmatrix} \tag{4}$$

$z_i = \nu_i \times \eta_i$

The propagation of forces on one link to another is represented by matrix $\phi(q) \in \mathbb{R}^{6n_d \times 6n_d}$.

$$\phi(q) = \begin{bmatrix} I & {}^2_1\hat{\phi}^T & {}^3_1\hat{\phi}^T & \cdots & {}^{n_d}_1\hat{\phi} \\ & I & {}^3_2\hat{\phi}^T & \cdots & {}^{n_d}_2\hat{\phi} \\ & & & \ddots & \\ 0 & & & & I \end{bmatrix} \tag{5}$$

$${}^i_j\hat{\phi} = \begin{bmatrix} {}^i_jR & \hat{p}_{\overline{ji}}\,{}^i_jR \\ 0 & {}^i_jR \end{bmatrix} \tag{6}$$

$$\begin{pmatrix} {}^1w_{1\Sigma} \\ {}^2w_{2\Sigma} \\ \vdots \\ {}^{n_d}w_{n_d\Sigma} \end{pmatrix} = \phi F \lambda \tag{7}$$

Where ${}^iw_{i\Sigma}$ is the total wrench from all features $(i,\ i+1, \cdots,\ n_d)$. ${}^i_j\hat{\phi}$ is the adjoint transform [11], which transforms a twist in reference frame j into an equivalent wrench in frame i. ${}^i_jR$ is the rotation matrix from i to j, $p_{\overline{ji}}$ is a vector from the origin of frame j to frame i, and $\hat{p}_{\overline{ji}}$ is matrix for the cross product with $p_{\overline{ji}}$. The matrix ϕ is sometimes called the Composite Rigid Body transformation for forces [6].

We may then express observed torques at each of the joints as:

$$\tau_d = \underbrace{S^T(q)\phi(q)F}_{C(q)}\lambda \tag{8}$$

$$S = \begin{bmatrix} {}^1s_1(q) & & & 0 \\ & {}^2s_2(q) & & \\ & & \ddots & \\ 0 & & & {}^{n_d}s_{n_d}(q) \end{bmatrix} \tag{9}$$

where ${}^is_i$ is the unit twist of the i-th joint. The *contact* Jacobian, C, gives the basis of all disturbance torques arising from the features f_i. Therefore all information related the configuration and geometry of the arm is in the contact Jacobian C and the actual contact that occurs is parameterized by λ.

3 Contact Localization

The contact Jacobian, C, is a $(n_d \times n_p)$ matrix, where n_p is the number of parameters in λ. In order to solve for τ_d using Eq. 8, we will have to make some assumptions on λ. Generically, the initial contact between the manipulator and the environment will occur at a single feature of the manipulator. Since this is the most important case for detecting and localizing collisions, we will focus on this case here. In the example above, the single contact assumption gives us 6 possible solutions, each corresponding to an over-determined 3×2 system of equations. Each contact hypothesis corresponds to taking a different subset of the columns of C. We will denote the reduced system obtained by taking the columns of C corresponding to feature i as C_i. We may then solve for $\lambda_i = C_i^{-1}\tau_d$, or if C_i is over-determined, then we may take the least squares solution $\lambda_i = \left(C^TC\right)^{-1}C^T\tau_d$.

Once we have determined a value for λ_i, the corresponding position on the link can be determined.

Proceedings of the International Conference on Intelligent Robots and Systems (IROS '95)
0-8186-7108-4/95 $10.00 © 1995 IEEE

For our example, the position of the link is given by $\mathbf{p}(\lambda_i) = \frac{\lambda_{i2}}{\lambda_{i1}} \in [0, L]$.

To determine which contact hypothesis best explains the observations, the contact state will be further analyzed as follows. In §3.1 we will check that the state of hypothesized contact is *admissible* given geometric and physical constraints. After this stage, it may be the case that more than one admissible hypothesis satisfies the constraints; in §3.2, we show how to construct a metric which compares the merit of the competing hypotheses to select an *optimal* hypothesis.

3.1 Constraints

The constraints on λ depend on the parameterization of the features. We will give the λ constraints for the example problem. The constraints for problems in 3D, or with the addition of friction will be marginally more complicated. Typical constraints include:

$\mathcal{C}_1$: Non-negative normal force. The contact forces can only be "outward" relative to the surface of the link.

$\mathcal{C}_2$: Geometric Constraints. The contact position must be on the link's surface.

$\mathcal{C}_3$: Frictional Constraints.

For our example the constraints are:

$$\mathcal{C}_1: \quad \lambda_{i1} \leq 0. \tag{10}$$

$$\mathcal{C}_2: \quad 0 \leq d = \frac{\lambda_{i2}}{\lambda_{i1}} \leq L. \tag{11}$$

where d is the position of the contact measured relative to Link_i's frame of reference.

The constraints can be treated as a filter to eliminate hypotheses after the computation of the parameters λ_i. However the constraints are typically linear inequalities, $A_i\lambda_i \leq 0$; (e.g., Equations 10,11). In this case the feasibility problem,

$$C_i\lambda_i = \tau_d \tag{12}$$

$$A_i\lambda_i \leq 0 \tag{13}$$

can be solved simultaneously using linear programming.

3.2 Feature Identification

In instances where there exists more than one admissible single-contact hypothesis which satisfies the constraints, we must use some means of determining which is most likely. For over-constrained problems, such as our example, a natural choice for ranking our solutions is the residual:

$$\text{proj}_i = \left|\left|\left(I - C_i\left(C_i^T C_i\right) C_i^T\right)\tau_d\right|\right|$$

the length of the projection of τ_d orthogonal to the column space of C_i. This is the sum of squared differences of the predicted and observed disturbance torques.

4 Results

To investigate the effectiveness of $proj_i$ as a feature classifier, a series of simulations involving the three DOF triangular-shaped manipulator were performed. A constant reaction force of $1N$ was used in generating the feature torques, with unit link lengths (L=1). The feature, f_i, was chosen randomly, as well as the position on the link. The joint angles q_2 and q_3 were chosen randomly from $[0, 2\pi]$. The ideal disturbance torques τ_d were computed, to which varying noise was added. The relative magnitude of the noise held constant at various levels $(0.01, 0.02, \cdots, 0.30)$. The direction of the error in $\mathbb{R}^3$ was uniformly distributed. In this way the error was uniformly distributed amongst the individual disturbance torques.

We measure success at classification in two ways: *feature identification* is measured by the percentage of contact features that are correctly classified; for each correctly identified feature, we measure the accuracy of *feature localization.*

Table 1 shows the effect of noise on the error rate of the feature identification. The error rates of the classification scheme utilizing the constraints C_i in conjunction with proj_i are very small; features were misclassified in less than 2% of the tests for relative errors in τ_d up to 30%. This indicates that proj_i is very effective in the identification of the feature involved in the collision, even when the disturbance torques contain a large relative error.

It should be noted that the error rates do not include contacts with features f_1 and f_2 on Link_1 (*i.e.,* only features $f_3, \cdots, f_6$). All simulated contacts on features f_1 and f_2 are wrongly classified as f_3 and f_4 respectively. This is due to the fact that a small error associated with the torque at q_2 will always produce an explanation of a collision on Link_2 very close to the proximal end of the link. Since the system is under-constrained for C_1 and C_2, any solution using the disturbance torques of $q_2, \cdots, q_{n_d}$ reflect only the noise. Features f_3 and f_4 are chosen rather than f_5, f_6 because we are looking for the smallest λ satisfying Eq(8). In practice, this can be easily dealt with; for example small disturbance torques at the distal joints of the manipulator can be set to zero or solutions with positions very close to the proximal end of the link can be rejected.

Since we have a large degree of confidence in the feature identification, we now turn our attention to the localization of the contact. The same method of constructing random collision examples was performed with the same noise models, and an estimate of each collision location was computed for each example. Only samples in which the correct feature was identified were considered. Additionally, only contacts involving $f_3, \cdots, f_6$ were considered since position cannot be recovered for collisions on the first link as it is underconstrained.

Proceedings of the International Conference on Intelligent Robots and Systems (IROS '95)
0-8186-7108-4/95 $10.00 © 1995 IEEE

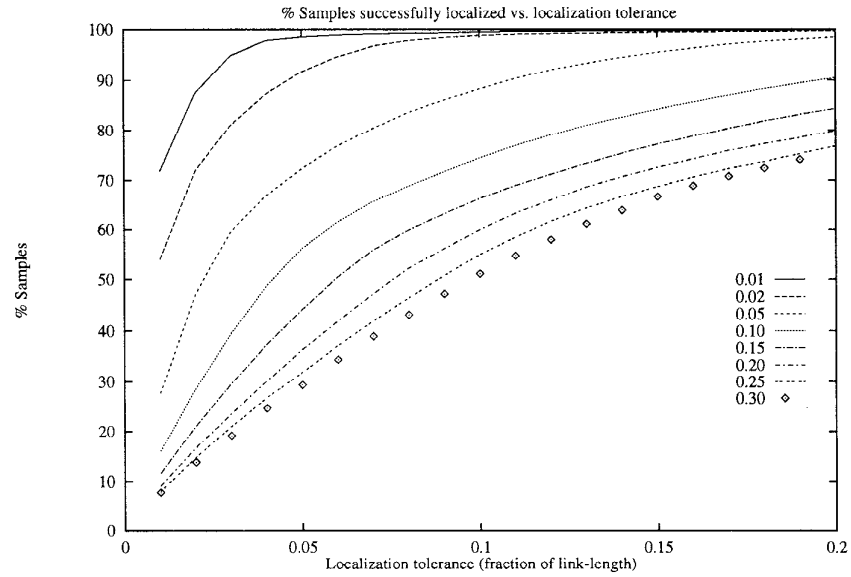

Figure 2: Cumulative distribution of localization errors for varying relative error in τ_d.

Relative Error $\frac{\|\tau_d - \tau_{ideal}\|}{\|\tau_d\|}$	Percentage Mis-classification
0.01	0.02
0.02	0.04
0.05	0.11
0.10	0.39
0.15	0.70
0.20	0.98
0.25	1.39
0.30	1.71

Table 1: Classification error rate with varying relative errors in τ_d.

Fig. 2 shows the effects of noise on the confidence level of our scheme in localizing the collision to various tolerances. Consider the task of resolving the collision to within 5% of its true value. We can see that our confidence level is is very high, 98.6% for 1% relative error, 91.7% for 2% relative error, and 72.3% for 5% relative error.

5 Extensions

We are currently investigating extensions of the above approach to include three-dimensional links, frictional forces, and links with curved surfaces. We briefly describe these extensions here. Three dimensional links and frictional forces can be modeled by extending the number of parameters for each feature. Curved link geometries are more difficult because of the non-linearities introduced.

For example, addition of friction to our two-dimensional problem adds an additional parameter, the component of reaction force tangent to the surface, as well as an additional frictional constraint. Thus

$$
\begin{aligned}
{}^{j}w_i &= \lambda_{i1} \begin{pmatrix} \eta_i \\ 0 \end{pmatrix} + \lambda_{i2} \begin{pmatrix} 0 \\ \nu_i \times \eta_i \end{pmatrix} \\
&\quad + \lambda_{i_3} \begin{pmatrix} \nu_i \\ 0 \end{pmatrix} \qquad (14) \\
C_4 &: \; -\mu \leq \frac{\lambda_{i3}}{\lambda_{i_1}} \leq \mu \qquad (15)
\end{aligned}
$$

where μ is the coefficient of friction. Since there are three parameters, we will may only determine the collision position for collisions with link 3 or higher.

Table 2 gives the number of parameters needed for various types of contact [10]:

Contact	2-D	3-D
Point contact without friction	2	3
Point contact with friction	3	5
Soft contact	3	6

Table 2: Contact Parameters

Thus for 3-dimensional frictional contacts we have 6 parameters. In general this will require that the

Proceedings of the International Conference on Intelligent Robots and Systems (IROS '95)
0-8186-7108-4/95 $10.00 © 1995 IEEE

contact occur on Link_i, $i \geq 6$, if we are to determine exactly the position of the contact. In some cases, this may restrict our ability to recover contact geometry. However, the increased number of constraints may sufficiently restrict the set of feasible contacts to still be of use for contacts on prior links. For some restricted applications we may have the required information to recover contact geometry exactly. For example, knowledge of the shape of the payload of a 6 or greater DOF manipulator will allow collisions of the payload with the environment to be recovered. This might be useful for teleoperation tasks for example.

The example we have been looking at has involved links whose surfaces are easy to parameterize. In some applications, links will have curved surfaces, leading to a feature matrix $F = F(\lambda)$ which is non-linear. This requires the solution of non-linear system of equations for λ_i. An alternative approach is to approximate the surface of the link by a series of polyhedral faces. This approximation can be hierarchical and successively refined, i.e., if a solution is feasible at given level of approximation, the face can be decomposed into smaller faces, and the process is repeated. Thus at each step we may eliminate a large fraction of the remaining surface of feasible contacts. The assumption that we are making is that while there may be localization inaccuracies due to the errors in approximating the normals of the surface with polygons, the positional information will be sufficient to constrain the position to a polygonal region. Results of the decomposition procedure are preliminary, but seem promising.

6 Conclusions

We have described a method by which unmodeled manipulator collisions can be identified, and the position of the contact can be localized. The method is based purely on the observed disturbance torques, and a set of features given by the geometry of the manipulator. The formulation provides an easy means of testing collision hypotheses, as well as a method for ranking competing hypotheses. We also describe extensions that are currently being investigated. Simulations of the method on a planar manipulator indicate that the method is robust with respect to noise for both collision feature identification, as well as feature localization.

References

[1] Antonio Bicchi, J. Kenneth Salisbury, and David L. Brock. Contact sensing from force measurments. *International Journal of Robotics Research*, 12(3):249–262, June 1993.

[2] R. A. Brooks. Solving the find-path problem by good representation of free space. *IEEE Trans. Systems, Man, and Cybernetics*, SMC-13(3):190–197, 1983.

[3] J. F. Canny. *The Complexity of Robot Motion Planning.* MIT Press, Cambridge, MA., 1993.

[4] B. R. Donald. *Error Detection and Recovery for Robot Planning with Uncertainty.* PhD thesis, MIT Department of Electrical Engineering and Computer Science, Cambridge, MA., 1987.

[5] Brian S. Eberman and J. Kenneth Salisbury. Determination of manipulator contact information from joint torque measurments. In Vincent Hayward and Oussama Khatib, editors, *Experminetal Robotics I: The First International Symposium, Montreal, June 19-21*, pages 463–473, 1989.

[6] A. Jain. Unified formulation of dynamics for serial rigid multibody systems. *Journal of Guidance, Control, and Dynamics*, 14(3):531–542, 1991.

[7] J. C. Latombe. *Robot Motion Planning.* Kluwer, 1991.

[8] T. Lozano-Peréz, M. T. Mason, and R. H. Taylor. Automatic synthesis of fine-motion strategies for robots. *Internal Journal of Robotics Research*, 3(1):3–24, 1987.

[9] Raashid Malik. Location by collision. In *Proceedings of the IEEE International Conference on Systems, Man and Cybernetics, V. 2*, pages 877–882, 1991.

[10] Matthew T. Mason and J. Kenneth Salisbury, Jr. *Robot Hands and the Mechanics of Manipulation.* MIT Press, Cambridge, MA., 1985.

[11] Richard M. Murray, Zexiang Li, and S. Shankar Sastry. *A Mathematical Introduction to Robot Manipulation.* CRC Press, Boka Raton, Fl., 1994.

[12] J. Kenneth Salisbury, Jr. Interpretation of contact geometries from force measurments. In Michael Brady and Richard Paul, editors, *Robotics Research: the First International Symposium.* MIT Press, Cambridge, MA., 1983.

[13] Shinji Takakura, Toshiyuki Murakami, and Kouhei Ohnishi. An approach to collision detection and recovery motion in industrial robot. In *Proceedings of the 1989 IEEE IECON*, pages 421–426, 1989.

Proceedings of the International Conference on Intelligent Robots and Systems (IROS '95)
0-8186-7108-4/95 $10.00 © 1995 IEEE